Transaction B: Mechanical Engineering
Vol. 16, No. 2, pp. 168–176

Research Note

Free Vibration Analysis of Rotating Laminated Cylindrical Shells Under Different Boundary Conditions Using a Combination of the Layerwise Theory and Wave Propagation Approach

S. Ramezani[1] **and M.T. Ahmadian**[1,*]

Abstract. *In this paper, vibration analysis of rotating laminated composite cylindrical shells using a combination of the layerwise theory and wave propagation approach is investigated. This combination enables us to study all the conventional boundary conditions in our analysis. Results obtained have been compared with those available in the literature and a good agreement has been observed. In contrast to the Equivalent Single Layer theories (ESL), the layerwise theory is constructed on the basis of C^0-continuity through the laminate thickness. For the surface of the shell, a displacement field based on the wave propagation approach is proposed. The effect of Coriolis and centrifugal accelerations on the circumferential and longitudinal modes is investigated. At high rotational speeds, the stationary frequency is smaller than both the forward and backward frequencies and this difference increases with the increase of rotational speed. The influence of boundary conditions on the frequencies is more significant at lower circumferential modes but at higher modes the effect of the boundary condition is infinitesimal.*

Keywords: *Rotating laminated cylindrical shells; Layerwise theory; Wave propagation.*

INTRODUCTION

Rotating shells and shafts are the main parts of many machines, such as gas turbines, locomotive engines and electric motors. In many cases, a rotating shell may be one of the main sources of vibration and noise. In order to reduce the vibration, noise and increasing strength, many shells and shafts are usually made of laminated composite materials. It is, therefore, very important for engineers to understand the vibration of composite shells in order to design suitable shells with low vibration and noise production characteristics.

Many studies have been carried out on rotating laminated cylindrical shells. Due to the mathematical complexity of obtaining analytical values for natural frequencies of laminated composite cylindrical shells, simple but reasonably accurate techniques are necessary and would be welcomed by the scientific community and industry.

Srinivasan and Lauterbach [1] obtained the natural frequency of a rotating cylinder by considering the effects of Coriolis forces and traveling modes. Zinberg and Symonds [2] experimentally obtained the critical speed of rotating cylindrical shells. The results also proved the advantages of using shells made of orthotropic materials over aluminum alloy shells. A finite element approach was used by dos Reis et al. [3] to obtain the critical speeds in the evaluation of the experiments of Zinberg and Symonds [2]. Traveling wave vibrations and the buckling of rotating anisotropic shells using a quasi-analytical finite element method have been studied by Padovan et al. [4]. A simplified theory for analyzing the first critical speed of a composite cylindrical shell was given by Kim and Bert [5] and a comparison with various shell theories was made. The free vibration analysis of a rotating

1. *Center of Excellence in Design, Robotic and Automation, Department of Mechanical Engineering, Sharif University of Technology, Tehran, P.O. Box 11155-9567, Iran.*
*. *Corresponding author. E-mail: ahmadian@sharif.edu*

Received 18 October 2006; accepted 26 December 2008

isotropic cylindrical shell using a harmonic reproducing kernel particle method is performed by Liew et al. [6]. Lam and Loy [7] extensively studied the vibrations of thin rotating cylindrical shells using different shell theories. Lam and Li [8] investigated rotating conical orthotropic shells based on Love's first approximation theory. The vibrations of rotating cross-ply and general laminated composite cylindrical shells based on Love's equations of motion and using a wave propagation approach have been investigated by Zhang [9-10]. A free vibration analysis of rotating cylindrical shells, using the layerwise laminate theory and only for simply supported boundary conditions has been performed by Kadivar and Samani [11].

In the present study, Reddy's layerwise theory [12,13] is combined with a wave propagation approach. This combination enables us to study all the conventional boundary conditions in our analysis. The layerwise theory based on C^0-continuity is constructed through the laminate thickness and the surface of the shell; a displacement field based on a wave propagation approach [9] is proposed and, hence, a combination of the layerwise theory and the wave propagation approach is obtained. Hamilton's principle is also used to derive the equations of motion.

Using this method, the effect of shell parameters on natural frequencies under various boundary conditions is investigated. One of the major advantages of the layerwise theory is the possibility it provides for analyzing thick laminates and, also, interlamina stresses (in forced vibrations) with high accuracy.

FORMULATION

Consider a laminated cylindrical shell with mean radius R, length L and thickness h. Let the shell be composed of several physical layers. Each physical layer is divided into arbitrary numerical layers. Assume that the total number of numerical layers is N, then, there would be $(N+1)$ numerical surfaces in the laminate. The shell is rotating about its horizontal axis at a constant angular speed, Ω. The reference surface of the shell is assumed to be at its middle surface where an orthogonal curvilinear coordinate system, (x, y, z), is fixed on this surface, as shown in Figure 1a. The displacement components of shell at time t are denoted by u, v and w, which are in the x-, y- and z-directions, respectively. As shown in Figure 1b, surface number 1 is located at $z_1 = -h/2$, while surface number $(N+1)$ is located at $z_{N+1} = h/2$. The k'th numerical layer lies between z_k and z_{k+1}.

Let $U_k(x, y)$, $V_k(x, y)$ and $W_k(x, y)$ be the displacement components of the kth surface in the x-, y- and z-directions, respectively. The displacement field may be approximated in the following form:

$$u(x, y, z, t) = U_k(x, y, t)\Phi_k(z),$$

$$v(x, y, z, t) = V_k(x, y, t)\Phi_k(z),$$

$$w(x, y, z, t) = W_k(x, y, t)\Phi_k(z). \tag{1}$$

Repeated indices indicate a summation from 1 to $N+1$ all through this paper. Furthermore, $\Phi_k(z)$ are global interpolation functions through the thickness of the laminate. Note that only C^0-continuity is required and, so Lagrangian interpolation functions may be used. Various degrees of Lagrangian interpolation functions of minimum order may be applied. The linear interpolation function can be constructed in the following form:

$$\Phi_k(z) = \begin{cases} 0 & \text{for } z \le z_{k-1} \\ (z_k - z)/t_{k-1} & \text{for } z_{k-1} \le z \le z_k \\ (z - z_k)/t_k & \text{for } z_k \le z \le z_{k+1} \\ 0 & \text{for } z \ge z_{k+1} \end{cases} \tag{2}$$

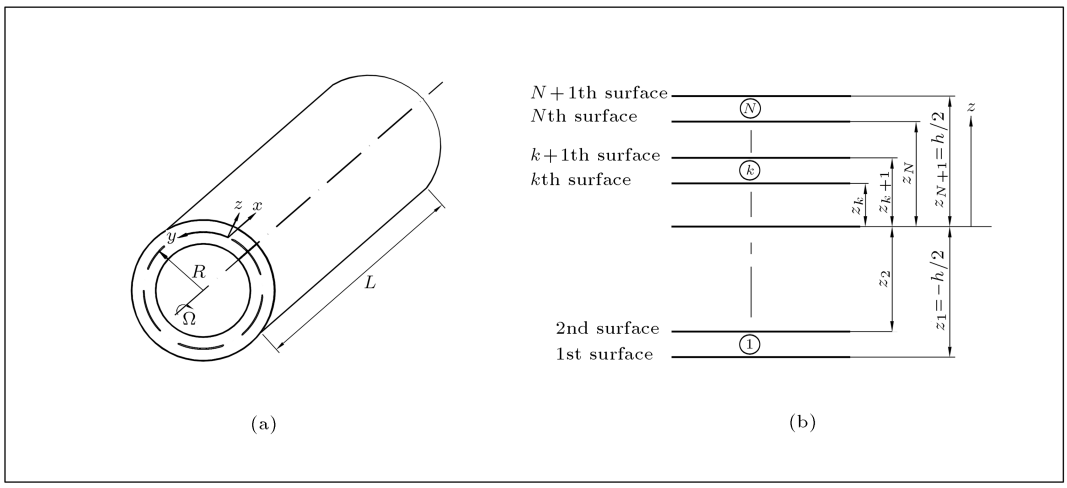

Figure 1. (a) Coordinate system; (b) Numerical layers and surfaces.

It is noted that $\Phi_k(z)$ takes the values between 0 and 1. Strain components in terms of displacement components may be written as:

$$\varepsilon_x = \frac{\partial u}{\partial x},$$

$$\varepsilon_z = \frac{\partial w}{\partial z},$$

$$\gamma_{xy} = \frac{\partial v}{\partial x} + \frac{1}{1+z/R}\frac{\partial u}{\partial y},$$

$$\varepsilon_y = \frac{1}{1+z/R}\left(\frac{\partial v}{\partial y} + \frac{w}{R}\right) + \frac{1}{2(1+z/R)^2}\left[\left(R\frac{\partial v}{\partial y} + \frac{w}{R}\right)^2 + \left(\frac{\partial u}{\partial y}\right)^2 + \left(\frac{\partial w}{\partial y} - \frac{v}{R}\right)^2\right],$$

$$\gamma_{yz} = \frac{1}{1+z/R}\left[\frac{\partial w}{\partial y} - \frac{v}{R} + (1+z/R)\frac{\partial v}{\partial z}\right],$$

$$\gamma_{xz} = \frac{\partial w}{\partial x} + \frac{\partial u}{\partial z}. \tag{3}$$

The terms in the bracket of ε_y denote the nonlinear terms of a Green-Saint Venat strain tensor. A different point of view on this subject is given in Liew et al. [6]. Hamilton's principle may be used for derivation of the equations of motion in the following form:

$$\int_{t_1}^{t_2} (\delta T - \delta\Pi)dt = 0, \tag{4}$$

where T is the kinetic energy and $\Pi = U - W$ is the total potential energy function, with U as strain energy and W as the work done by external forces. The velocity vector at each point of the shell may be written as:

$$\vec{V} = \vec{V}_{\rm rel} + \vec{\Omega}\times\vec{r} = \dot{u}\hat{e}_1 + [\dot{v} - \Omega(R+w)]\hat{e}_2 + (\dot{w} + \Omega v)\hat{e}_3, \tag{5}$$

where $(\dot{\cdot})$ denotes differentiation, with respect to time t, and $\hat{e}$ are unit vectors. Variation of the kinetic energy, strain energy and the work of external forces may be written as:

$$\delta U = \iiint_{\rm vol} (\sigma_x\delta\varepsilon_x + \sigma_y\delta\varepsilon_y + \sigma_y\delta\varepsilon_y + \sigma_{xy}\delta\gamma_{xy} + \sigma_{xz}\delta\gamma_{xz} + \sigma_{yz}\delta\gamma_{yz})dV, \tag{6a}$$

$$\delta T = \iiint_{\rm vol} \rho\vec{V}.\delta\vec{V}\,dV, \tag{6b}$$

$$\delta W = -\iint_{\text{top surface}} P_z(x,y)\delta W_{N+1}(x,y)dA_{\rm external}, \tag{6c}$$

where $P_z(x,y)$ is the distributed load on the external surface. The volume and external area elements are $dV = (1+z/R)dxdydz$ and $dA_{\rm external} = (1+h/2R)dxdy$, respectively. Next, let us introduce the following generalized stress resultants:

$$M_x^k = \int_{-h/2}^{h/2} \sigma_x(1+z/R)\Phi_k dz,$$

$$M_y^k = \int_{-h/2}^{h/2} \sigma_y\Phi_k dz,$$

$$N_z^k = \int_{-h/2}^{h/2} \sigma_z(1+z/R)\Phi_k' dz,$$

$$R_y^k = \int_{-h/2}^{h/2} \sigma_{yz}\Phi_k dz,$$

$$R_x^k = \int_{-h/2}^{h/2} \sigma_{xz}(1+z/R)\Phi_k dz,$$

$$Q_x^k = \int_{-h/2}^{h/2} \sigma_{xz}(1+z/R)\Phi_k' dz,$$

$$Q_y^k = \int_{-h/2}^{h/2} \sigma_{yz}(1+z/R)\Phi_k' dz,$$

$$M_{xy}^k = \int_{-h/2}^{h/2} \sigma_{xy}(1+z/R)\Phi_k dz,$$

$$M_{yx}^k = \int_{-h/2}^{h/2} \sigma_x\Phi_k dz,$$

$$\overline{N} = R^2(1+z/R)^2\Omega^2\int_{-h/2}^{h/2}\rho dz, \tag{7}$$

where the prime symbol $(')$ denotes differentiation, with respect to z. From Equations 1 to 3, 6 and 7,

we have:

$$\delta T = \iint_{\text{Area}} \{\dot{U}_k \delta \dot{U}_j + [\dot{V}_k - \Omega(R + W_k)][\delta \dot{V}_j - \Omega(R + \delta W_j)] + (\dot{W}_k + \Omega V_k)(\delta \dot{W}_j + \Omega \delta V_j)\} I_{jk} dx dy, \tag{8a}$$

$$\delta U = \iint_{\text{Area}} \left[M_x^k \frac{partial(\delta U_k)}{\partial x} + M_y^k \frac{\partial(\delta V_k)}{\partial y} + \left(\frac{1}{R} M_y^k + N_z^k\right) \delta W_k + \left(Q_y^k - \frac{1}{R} R_y^k\right) \delta V_k + R_y^k \frac{\partial(\delta W_k)}{\partial y} + R_x^k \frac{\partial(\delta W_k)}{\partial x} + Q_x^k \delta U_k + M_{xy}^k \frac{\partial(\delta V_k)}{\partial x} + M_{yx}^k \frac{\partial(\delta U_k)}{\partial y} + \frac{\overline{N}}{(1 + z/R)^2} \left[\frac{\partial U_k}{\partial y} \delta \left(\frac{\partial U_k}{\partial y} \right) + \left(R \frac{\partial V_k}{\partial y} + \frac{W_k}{R} \right) \left(R \delta \frac{\partial V_k}{\partial y} + \frac{\delta W_k}{R} \right) + \left(\frac{\partial W_k}{\partial y} - \frac{V_k}{R} \right) \left(\delta \frac{\partial W_k}{\partial y} - \frac{\delta V_k}{R} \right) \right] \right] dx dy, \tag{8b}$$

where the generalized inertia components, I_{jk}, are defined as:

$$I_{jk} = \int_{-h/2}^{h/2} \rho(1 + z/R) \Phi_j \Phi_k dz. \tag{9}$$

Now, assuming $P_z(x, y) = 0$ and applying the fundamental lemma of calculus of variations, the equations of motion may be found from Equation 4 in the following form:

$$I_{jk} U_{k,tt} = M_{x,x}^k + M_{yx,y}^k - Q_x^k + I_{jk} R^2 \Omega^2 U_{k,yy}, \tag{10a}$$

$$I_{jk}[V_{j,tt} - 2\Omega W_{j,t} - \Omega^2 V_j] = M_{xy,x}^k + M_{y,y}^k - Q_y^k + \frac{R_y^k}{R} + I_{jk} R^2 \Omega^2 \left[V_{j,yy} + \frac{2W_{j,y}}{R} - \frac{V_j}{R^2} \right], \tag{10b}$$

$$I_{jk}[W_{j,tt} + 2\Omega V_{j,t} - \Omega^2 W_j] = R_{x,x}^k + R_{y,y}^k - N_z^k - \frac{M_y^k}{R} + I_{jk} R^2 \Omega^2 \left[W_{j,yy} - \frac{2V_{j,y}}{R} - \frac{W_j}{R^2} \right]. \tag{10c}$$

In order to express the generalized stress resultants in terms of displacement components from 3-D Hooke's law we have:

$$\begin{Bmatrix} \sigma_x \\ \sigma_y \\ \sigma_z \\ \sigma_{yz} \\ \sigma_{xz} \\ \sigma_{zx} \end{Bmatrix}^{(i)} = \begin{bmatrix} \overline{C}_{11} & \overline{C}_{12} & \overline{C}_{13} & 0 & 0 & \overline{C}_{16} \\ & \overline{C}_{22} & \overline{C}_{23} & 0 & 0 & \overline{C}_{26} \\ & & \overline{C}_{33} & 0 & 0 & \overline{C}_{36} \\ & & & \overline{C}_{44} & \overline{C}_{45} & 0 \\ & \text{sym} & & & \overline{C}_{55} & 0 \\ & & & & & \overline{C}_{66} \end{bmatrix}^{(i)} \begin{Bmatrix} \varepsilon_x \\ \varepsilon_y \\ \varepsilon_z \\ \varepsilon_{yz} \\ \varepsilon_{xz} \\ \varepsilon_{zx} \end{Bmatrix}^{(i)}, \tag{11}$$

where upper index (i) denotes the i'th numerical layer. From Equations 1, 2, 7 and 11 we obtain:

$$M_x^k = D_{11}^{kj} U_{j,x} + D_{12}^{kj} \left(V_{j,y} + \frac{W_j}{R} \right) + B_{13}^{kj} W_j + D_{16}^{kj} V_{j,x} + \overline{D}_{16}^{kj} U_{j,y}, \tag{12a}$$

$$M_y^k = \overline{D}_{12}^{kj} U_{j,x} + \tilde{D}_{22}^{kj} \left(V_{j,y} + \frac{W_j}{R} \right) + \overline{B}_{23}^{kj} W_j + \overline{D}_{16}^{kj} V_{j,x} + \tilde{D}_{16}^{kj} U_{j,y}, \tag{12b}$$

$$N_z^k = B_{13}^{jk} U_{j,x} + \overline{B}_{23}^{jk} \left(V_{j,y} + \frac{W_j}{R} \right) + A_{33}^{kj} W_j + B_{36}^{jk} V_{j,x} + \overline{B}_{36}^{jk} U_{j,y}, \tag{12c}$$

$$R_x^k = \overline{D}_{45}^{jk} \left(W_{j,y} - \frac{V_j}{R} \right) + B_{45}^{kj} V_j + D_{55}^{kj} W_{j,x} + B_{55}^{kj} U_j, \tag{12d}$$

$$R_y^k = \tilde{D}_{44}^{kj} \left(W_{j,y} - \frac{V_j}{R} \right) + \overline{B}_{44}^{kj} W_{j,x} + \overline{D}_{45}^{kj} W_{j,x} + \overline{B}_{45}^{kj} U_j, \tag{12e}$$

$$Q_x^k = \overline{B}_{45}^{jk} \left(W_{j,y} - \frac{V_j}{R} \right) + A_{55}^{jk} U_j + A_{45}^{kj} V_j + B_{55}^{jk} W_{j,x}, \tag{12f}$$

$$Q_y^k = \overline{B}_{44}^{jk} \left(W_{j,y} - \frac{V_j}{R} \right) + A_{44}^{kj} V_j + B_{45}^{jk} W_{j,x} + A_{45}^{jk} U_j, \tag{12g}$$

$$M_{xy}^k = D_{66}^{kj} V_{j,x} + \overline{D}_{66}^{kj} U_{j,y}, \tag{12h}$$

$$M_{yx}^{k} = \overline{D}_{66}^{kj} V_{j,x} + \tilde{D}_{66}^{kj} U_{j,y}, \tag{12i}$$

where the coefficients A_{pq}^{kj}, B_{pq}^{kj}, D_{pq}^{kj}, $\overline{B}_{pq}^{kj}$, $\overline{D}_{pq}^{kj}$ and $\tilde{A}_{pq}^{kj}$ are defined as:

$$(A_{pq}^{kj}, B_{pq}^{kj}, D_{pq}^{kj}) = \sum_{i=1}^{N} \int_{z_i}^{z_{i+1}} \overline{C}_{pq}^{(i)} (1 + z/R) \cdot (\Phi_k' \Phi_j', \Phi_k \Phi_j', \Phi_k \Phi_j) dz, \tag{13a}$$

$$(\overline{B}_{pq}^{kj}, \overline{D}_{pq}^{kj}) = \sum_{i=1}^{N} \int_{z_i}^{z_{i+1}} \overline{C}_{pq}^{(i)} \cdot (\Phi_k \Phi_j', \Phi_k \Phi_j) dz, \tag{13b}$$

$$\tilde{D}_{pq}^{kj} = \sum_{i=1}^{N} \int_{z_i}^{z_{i+1}} \overline{C}_{pq}^{(i)} \Phi_k \Phi_j / (1 + z/R) dz. \tag{13c}$$

It is noted that the integration is performed between numerical layers. By calculating Equation 13 and substituting Equations 12 into Equation 9, the governing equations of motion may be obtained.

In the next step, using a wave propagation approach, we introduce the proper displacement field for the problem.

WAVE PROPAGATION APPROACH

The displacements of the shell may also be expressed in the format of wave propagation, associated with axial wave number K_m (m represents axial wave number) and circumferential modal parameter n, denoted by:

$$\begin{cases} U_k(x,y,t) = \overline{U}_k e^{(i\omega t - iK_m x - iny/R)} \\ V_k(x,y,t) = \overline{V}_k e^{(i\omega t - iK_m x - iny/R)} \\ W_k(x,y,t) = \overline{W}_k e^{(i\omega t - iK_m x - iny/R)} \end{cases} \tag{14}$$

where $\overline{U}_k$, $\overline{V}_k$ and $\overline{W}_k$ are amplitudes of vibration in (m,n) mode. Substituting Equations 14 into Equations 10 gives the following system of equations:

$$[S(\omega)]_{3(N+1)\times 3(N+1)} \{\overline{U}_1 \overline{V}_1 \overline{W}_1 \cdots \overline{U}_{N+1} \overline{V}_{N+1} \overline{W}_{N+1}\}^t_{3(N+1)\times 1} = \{0\}. \tag{15}$$

For nontrivial solutions, the determinant of the characteristic matrix, $[S(\omega)]$, must be zero, which results in $3(N+1)$ frequencies of the system for each given pair of (m,n) values.

The appropriate axial wave number, K_m, should be chosen, so that Equations 14 satisfies the required boundary conditions at both ends of the cylindrical shell. In the wave propagation approach, the wave traveling in the axial direction of the shell can be approximated as the wave traveling in a similar beam [9]. This notion enables us to simply estimate the flexural vibration of the cylindrical shell. The values of $K_m L$ in the flexural vibration of beam for various boundary conditions are summarized in Table 1. These results may be easily obtained by solving the eigenvalue problem of the vibration of an Euler-Bernoulli beam with corresponding boundary conditions. In Table 1, some abbreviations are used for different boundary conditions. For example, F/F denotes both end free boundary conditions.

For the beam under different boundary conditions, in lower modes of vibration, the values of $K_m L$ given in Table 1 are slightly different from the exact values. But the error is negligible except for the case of SS/SS beams, the wave number for which is exactly the same as analytical values. However, in higher modes of vibration, all values of $K_m L$ may be regarded as exact values. Wave numbers given in this table are used in our analysis.

Table 1. Approximate values of wave numbers for different BC's [9].

Boundary Conditions	Wave Numbers ($K_m L$)
Free/Free (F/F)	$(2m+1)\pi/2$
Free/Sliding (F/S)	$(4m-1)\pi/4$
Clamped/Free (C/F)	$(2m-1)\pi/2$
Free/Simply Supported (F/SS)	$(4m+1)\pi/4$
Simply Supported/Simply Supported (SS/SS)	$m\pi$
Clamped/Simply Supported (C/SS)	$(4m+1)\pi/4$
Clamped/Clamped (C/C)	$(2m+1)\pi/2$
Clamped/Sliding (C/SL)	$(4m-1)\pi/4$
Sliding/Sliding (SL/SL)	$m\pi$
Sliding/Simply Supported (SL/SS)	$(2m-1)\pi/2$

NUMERICAL RESULTS AND DISCUSSION

To check the accuracy of the present analysis, the results obtained are compared with those in the literature. The cylindrical shells considered are three-layered, cross-ply, laminated cylindrical shells with symmetric lamination about the middle surface and a [90/0/90] stacking sequence. Through all analyses, by dividing each physical layer into two numerical layers sufficient accuracy in convergence is obtained. The thickness of all layers is equal, being one-third of the shell thickness. Mechanical properties of the shell material are given in Table 2.

The non-dimensional frequency parameter is defined as $\omega^* = R\omega\sqrt{\rho_0/E_{22}}$ where ρ_0 is the density per unit volume and E_{22} is the Young's modulus of elasticity in the second principal direction. The non-dimensional natural frequencies obtained in this analysis are compared with those by Lam and Loy [7] and Zhang [9]. In Table 3, the effect of the rotational speed, Ω, for the cylindrical shell with SS/SS boundary conditions and $h/R = 0.002$, $L = R = 1$ is presented. Comparing the findings in this paper with the results in the literature indicates a good agreement with an accuracy of 1 to 2 percent. The fordward and backward frequencies are investigated with a change in the rotating angular velocity, Ω, in Figure 2 with $h/R = 0.002$, $L = 1$, $L/R = 10$ and $(m, n = (1, 1)$. As the angular velocity, Ω, increases, the forward frequency reduces, but the backward frequency increases monotonically. The difference between the forward and backward frequencies increases with the increase of angular velocity, Ω. It is interesting to note that the intersection of the forward frequency curve with the Ω-axis is the so called critical speed of rotor corresponding to a $(m, n) = (1, 1)$ mode, in which the rotating speed and the speed of the forward whirl coincide.

Variations of the backward, forward and stationary non-dimensional frequency, ω^*, with the circumferential mode, n, under C/C-boundary conditions and $h/R = 0.002$, $L = 1$, $L/R = 10$, $m = 1$ and

Table 2. Mechanical properties of the shell material.

E_{11}	19 GPa	E_{22}	7.6 GPa	E_{33}	7.6 GPa
G_{12}	4.1 Gpa	G_{13}	4.1 Gpa	G_{23}	1.4 Gpa
v_{12}	0.26	v_{13}	0.26	v_{23}	0.37
ρ_0	1643 kg/m^3				

Table 3. Comparison of the non-dimensional frequency ω^* for [90/0/90] arrangement with SSSS boundary conditions in different rotating speeds ($h/r = 0.002$, $m = 1$ and $L = R = 1$).

Ω	n	Zhang [1]		Lam & Loy [3]		Present Method	
		ω_b^*	ω_f^*	ω_b^*	ω_f^*	ω_b^*	ω_f^*
0.1	1	1.061428	1.016139	1.061429	1.061140	1.088543	1.078262
	2	0.804213	0.803892	0.804214	0.803894	0.779242	0.779147
	3	0.598473	0.598185	0.598476	0.598187	0.563771	0.563712
	4	0.450266	0.450017	0.450270	0.450021	0.416606	0.416506
	5	0.345358	0.345144	0.345363	0.345149	0.318704	0.318678
	6	0.270845	0.270660	0.270852	0.270667	0.249507	0.249459
0.4	1	1.061861	1.060705	1.061862	1.060706	1.084906	1.078309
	2	0.804695	0.803414	0.804696	0.803415	0.779217	0.779210
	3	0.598913	0.597759	0.598915	0.597762	0.563706	0.563704
	4	0.450658	0.449663	0.450662	0.449667	0.416648	0.416626
	5	0.345719	0.344865	0.345724	0.344870	0.318580	0.318657
	6	0.271200	0.270461	0.271207	0.270468	0.249600	0.249600
1.0	1	1.062727	1.059835	1.062728	1.059836	1.086192	1.077931
	2	0.805665	0.802462	0.805667	0.802464	0.778677	0.778993
	3	0.599817	0.596934	0.599820	0.596937	0.563061	0.563398
	4	0.451509	0.449023	0.451513	0.449027	0.416339	0.416593
	5	0.346588	0.344453	0.346593	0.344459	0.316836	0.317099
	6	0.272190	0.270343	0.272197	0.270349	0.252652	0.252880

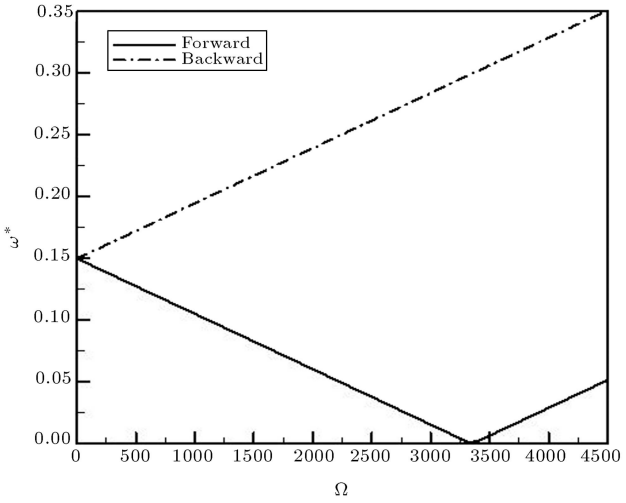

Figure 2. Variation of ω^* with the angular speed Ω (rps) and CC boundary conditions ($h/r = 0.002$, $L = 1$, $L/R = 10$ and $(m, n) = (1, 1)$).

$\Omega = 200$ rps are shown in Figure 3. For small values of Ω, the differences between the forward, backward and stationary frequencies are very small for all values of n, while as Ω increases, the differences between the frequencies increase.

The backward frequency is investigated with different boundary conditions in Figure 4 with $h/R = 0.002$, $L = 1$, $L/R = 10$, $m = 1$ and $\Omega = 5$ rps varying with the circumferential mode, n, for four different boundary conditions. A similar diagram may be obtained for the corresponding forward frequencies. The boundary conditions considered are C/C, C/SS, SS/SS and C/SL. The effect of boundary conditions are

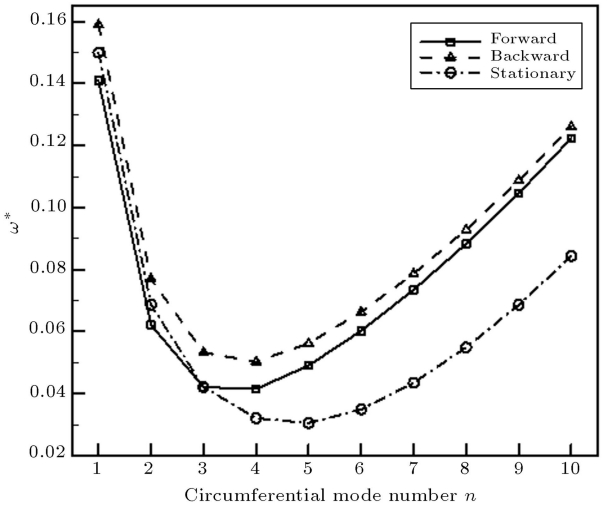

Figure 3. Variation of the backward, forward and stationary non-dimensional frequency ω^* with the circumferential mode number n and CC boundary conditions, ($h/r = 0.002$, $L = 1$, $L/R = 10$, $m = 1$ and $\Omega = 200$ rad/s).

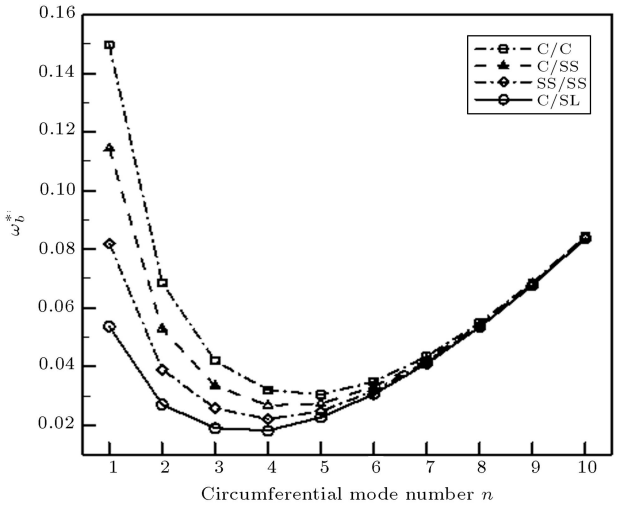

Figure 4. Variation of the backward non-dimensional frequency ω_b^* with the circumferential mode n and various boundary conditions ($h/r = 0.002$, $L = 1$, $L/R = 10$, $m = 1$ and $\Omega = 5$).

observed to be more significant at lower circumferential mode numbers, while at high circumferential mode numbers, n, this effect is not important. In fact, there is hardly any influence of boundary conditions at high circumferential modes. In Figure 4, the C/C boundary conditions have the highest forward and backward natural frequencies at lower circumferential modes, followed by C/SS, SS/SS and C/SL boundary conditions.

Figure 5 shows the forward frequencies versus thickness parameter h/R with the C/C boundary conditions and $L/R = 10$, $m = 1$ and $\Omega = 100$ rps. The frequencies for $n = 1, 2$ and 3 are presented. Value of h/R varies between 0.005 and 0.05. For the case where $n = 3$, the frequencies increase monotonically

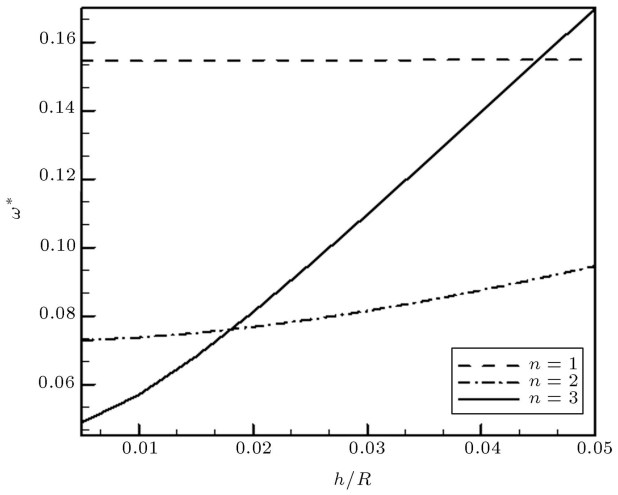

Figure 5. Variation of ω^* with the h/R ratio and CC boundary conditions, ($L = 1$, $L/R = 10$, $m = 1$ and $\Omega = 100$).

as h/R increases. As the circumferential mode number decreases to $n = 2$, the frequency growth rate decreases dramatically, while for $n = 1$ the frequencies remain nearly unchanged. It should be noted that at $h/R = 0.018$, the third and second circumferential modes of vibration are superimposed. It is interesting to note that in harmonic excitation, as frequency of excitation increases for $h/R < 0.018$, the third mode of the circumferential vibration will be excited prior to the second modes while for $h/R > 0.018$, the excitation will be in reverse order.

The forward, stationary and backward frequencies are plotted versus L/R ratios for $R = 1$, $h/R = 0.005$, $\Omega = 100$ rps, $(m, n) = (1, 1)$ and CC boundary conditions in Figure 6. It is observed that as length parameter L/R increases the frequencies decrease. However, the rate of the frequency reduction is much higher at larger values of L/R. As L/R increases, the forward and backward frequencies diverge from one another, while the stationary frequency remains within the limits of the forward and backward frequencies.

CONCLUSIONS

The vibration analysis of laminated composite cylindrical shells using a method based on a combination of the layerwise theory and the wave propagation approach is presented. Natural frequencies resulted by this method are in good agreement with those available in the literature. Effects of shell parameters, m, n, h/R, L/R, and angular velocity, Ω, at different boundary conditions on the natural frequencies, are investigated. At low circumferential modes (small n values), the stationary natural frequencies are between the forward and backward frequencies, while at high circumferential modes (large n values), the stationary frequency is smaller than both forward and backward natural frequencies. This means that mode number n has more influence than angular speed, Ω, on the forward and backward frequencies at low circumferential modes. But at high circumferential modes, angular speed, Ω, plays a leading role on the forward and backward frequencies rather than mode number n. This is due to the effectiveness of Coriolis and centrifugal forces at high rotating speeds. The backward frequency is always larger than the forward frequency; however, the difference between the backward and forward frequencies reduces as mode n increases. The backward frequency increases monotonically with the increase of angular speed while the forward frequency decreases at smaller (m, n) modes and increases at larger (m, n) modes. However, the difference between the forward and backward frequencies grows with the increase of angular velocity. The effect of boundary conditions on the natural frequencies is significant at low circumferential modes while at high circumferential modes, forward, backward and stationary frequencies are independent of imposed boundary conditions. The transition of fundamental frequencies from higher to lower circumferential modes occurs at different h/R ratios for different boundary conditions. The natural frequencies decrease as the length parameter, L/R, increases, but the reductions are significant at low L/R ratios. For any length parameter L/R ratios, the stationary frequencies are between the forward and backward frequencies. The difference between the forward and backward frequencies enhances as L/R increases. It has been noted that natural frequencies decrease sharply at low values of L/R, but this variation is smooth at large L/R ratios. The stationary natural frequency is between forward and backward frequencies for all length parameters, L/R. The differences between forward and backward frequencies enhance as L/R increases.

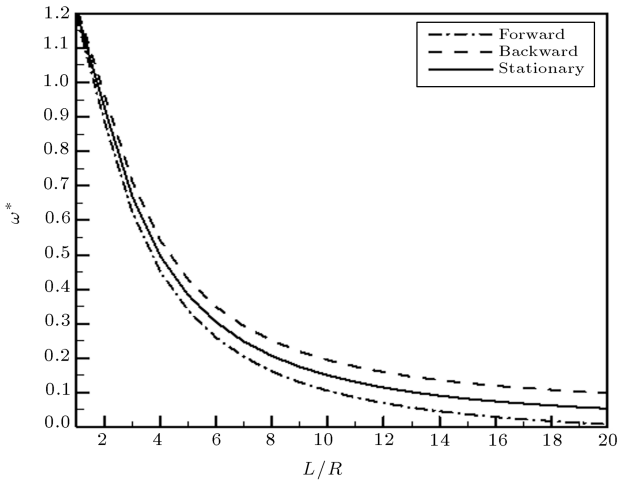

Figure 6. Variation of ω^* with the ratio for [90/0/90] with CC boundary conditions ($R = 1$, $h/r = 0.005$, $Omega = 100$ and $(m, n) = (1, 1)$).

REFERENCES

1. Srinivasan, A.V. and Lauterbach, G.F. "Travelling waves in rotating cylindrical shells", *ASME Journal of Engineering for Industry*, **93**, pp. 1229-32 (1971).

2. Zinberg, H. and Symonds, M.F. "The development of advanced composite tail rotor driveshaft", *26th Annual Forum of the American Helicopter Society*, pp. 1-14 (1979).

3. dos Reis, H.L.M., Goldman, R.B. and Verstrate, P.H. "Thin-walled laminated composite cylindrical tubes: Part III - critical speed analysis", *Journal of Composites Technology and Research*, **9**, pp. 58-62 (1987).

4. Padovan, J. "Traveling waves vibrations and buckling of rotating anisotropic shells of revolution by finite elements", *International Journal of Solids and Structures*, **11**, pp. 1367-1380 (1975).

5. Kim, C.D. and Bert, C.W. "Critical speed analysis of laminated composite, hollow drive shafts", *Composite Engineering*, **3**, pp. 633-43 (1993).
6. Liew, K.M., Ng, T.Y., Zhao, X. and Reddy, J.N. "Harmonic reproducing kernel particle method for free vibration analysis of rotating cylindrical shell", *Computer Methods in Applied Mechanics and Engineering*, **191**, pp. 4141-4157 (2002).
7. Lam, K.Y. and Loy, C.T. "Analysis of rotating laminated cylindrical shells by different thin shell theories", *Journal of Sound and Vibration*, **186**, pp. 23-35 (1995).
8. Lam, K.Y. and Li, H. "On free vibration of rotating truncated circular orthotropic conical shell", *Composites Part B*, **30**, pp. 135-144 (1999).
9. Zhang, X.M. "Parametric analysis of frequency of rotating laminated composite cylindrical shells with the wave propagation approach", *Computer Methods in Applied Mechanics and Engineering*, **191**, pp. 2029-2043 (2002).
10. Zhang, X.M. "Vibration analysis of cross-ply laminated composite cylindrical shells using the wave propagation approach", *Applied Acoustics*, **62**, pp. 1221-1228 (2001).
11. Kadivar, M.H. and Samani, K. "Free vibration of rotating thick composite cylindrical shells using layerwise laminated theory", *Mechanics Research Communications*, **27**, pp. 679-684 (2000).
12. Reddy, J.N., *Mechanics of Laminated Composite Plates and Shells, Theory and Analysis*, 2nd edition, CRC press (2003).
13. Nosier, A., Kapania, R.K. and Reddy, J.N. "Free vibration analysis of laminated plates using layerwise theory", *AIAA Journal*, **31**, pp. 2335-2346 (1993).